**ACADEMICIA: An International Multidisciplinary Research Journal**
ISSN: 2249-7137 Vol. 16 Issue 1, January, 2026 SJIF 2022= 8.252
A peer reviewed journal

# A COMPARATIVE STUDY OF DIFFERENT GAS CHANNEL STRUCTURES INPERFORMANCE DEGRADATION OFPROTON EXCHANGE MEMBRANE FUEL CELL

**Abhilasha Singh*; Prateek Arora**; Kripa Shanker Singh***; BP Singh****; Purushottam Kumar*****

*Department of Physics,
Raja BalwantSingh College,
Dr. Bhimrao Ambedkar University,
Paliwal Park Agra, INDIA
Email id: abhilasha.bah@gmail.com

**Department of Physics,
IBS Khandari Campus,
Dr. Bhimrao Ambedkar University,
Paliwal Park Agra, INDIA

**DOI: 10.5958/2249-7137.2026.00002.7**

## ABSTRACT

*The electrochemical performance and durability of proton exchange membrane fuel cells (PEMFCs) are strongly governed by the geometry and topology of the reactant flow field. In particular, the gas channel configuration plays a critical role in regulating reactant distribution, water management, pressure drop and interfacial mass transport between the gas diffusion layer (GDL) and the catalyst layer. PEMFCs generally exhibit enhanced current density and improved polarization characteristics when a larger fraction of the gas flow channel area is in direct contact with the GDL, thereby promoting more uniform reactant utilization and reduced concentration overpotentials. In the present study, a comparative numerical investigation of different gas channel structures and their influence on PEMFC performance degradation was conducted using COMSOL Multiphysics. Two alternative gas flow channel geometries with identical inlet and outlet cross-sectional areas but differing channel–GDL contact areas were developed and analyzed. A conventional rectangular (cuboidal) parallel flow field and a cylindrical parallel flow field design were selected to systematically assess the impact of channel geometry on electrochemical and transport phenomena. We investigated and observed the hydrogen mass fraction, ionic potential and electronic potential include the oxygen, nitrogen, water mass fractionsand the current density across the membrane. The velocity field vectors and the pressure in the anode and cathode compartments is also studied.For a rectangular (cuboidal) structure, it displays better results for pressure, velocity and membrane current density.*

**KEYWORDS:** *Topology,Cylindrical Channel, Rectangular (Cuboidal) Channel, Ionic Density, Boundary, Pressure, PEMFC.*

## INTRODUCTION

Due to the fact that conventional energy sources cannot produce enough energy, alternatives to them must also be taken into account together with the rising energy consumption. To lessen the negative effects of generating energy from fossil fuels and other conventional sources, the development of clean and sustainable energy has become essential worldwide [1]. These kinds of energy sources are referred to be alternative energy sources among the different alternative energy sources. The fuel cell is one of the alternatives on this list of alternative energy sources. The most efficient and dependable option with regards to energy conversion technology is the fuel cell. In 1839 American scientist and lawyer William Grove constructed the first quiet basic fuel cell [2]. Two platinum electrodes made up this instrument [3]. Grove's innovation was enhanced by Charles Langer and Ludwig Mond in 1889 by employing a porous mono-conductive electrolyte. Fuel cells are the current name for this technology [4, 5]. A fuel cell is a device that uses electrochemical processes, such as anodic oxidation and catholic reduction reactions, to transform the chemical energy of hydrogen fuel into electricity and create water. When burned with oxygen, hydrogen fuel produces no emissions. Fuel cells is capable of providing long-term answers as efficient and sustainable energy conversion technologies that emit little or no greenhouse gases [6]. Fuel cell classification and features are described based on the electrolyte employed. The various fuel cell types include alkaline fuel cells (AFCs), molten carbonate fuel cells (MCFCs), phosphoric acid fuel cells (PAFCS), solid oxide fuel cells (SOFCs), and proton exchange membranes fuel cells (PEMFCs).

The layout'ssimplicityand operating set-up of thePEMFCmakes it an acceptable replacement energy source. PEMFC systems have appealing qualities such their light weight, greatest energy density, minimal pollutant output, and low operating temperature. The operating set-up, mechanical design, transport mechanisminside the cells, manufacturing process, and rate of electrochemical reactions all have a significant impact on PEMFC cell performance. Anode and cathode PEMFC chemical processes are

**Anode:** Hydrogen undergoes oxidation to form protons as shown below.

$$2H_2 \rightarrow 4H^+ + 4\,e^- \quad (1)$$

Energy is released in this reaction. At the cathode, the oxygen interacts with theelectrolyte's $H^+$ ions and the electrons ($e^-$) released from the electrode. Water is created as a result of this.

**Cathode:** Oxygen undergoes reduction to from water as given below.

$$O_2 + 4e^- + 4H^+ \rightarrow 2H_2O \quad (2)$$

The hydrogen fuel is burned or undergoes a simple reaction in the entire process [7, 8], which occurs as follows.

$$2H_2 + O_2 \rightarrow 2H_2O \quad (3)$$

The most promising energy converters are PEM fuel cells, particularly for automotive applications. They can be employed in clean hybrid electricity systems and deliver the load with rated power [9, 10]. The restricted use of the PEMFCsare its high economic expenses, durability and fuel availability issues, or the challenge of maintaining effective thermal control. Water management also has a substantial impact on fuel cell efficiency [11, 12]. Membrane dehydrates, when the water removal rate exceedsthe rate of water formation. This results in substantial ohmic voltage drops within the cell, which reduces the performance of Fcs [13].

Between the BPs and the CLs lie porous medium called the GDLs.As a result, they not only enable the uniform distribution of the reactants across the surface of the CLs, but they also create a structural support for the catalyst layers and enable an electrical link (electrons transit) between the catalyst layers and the bipolar plates [14].Although cylindrical configurations have been developed, channels typically have a rectangular structure and shape. The fuel and oxidant flow rates, as well as the water accumulation in the cell, can be impacted by changes in channel form. Condensed water consequently forms a film at the bottom of flow channels that are spherical, whereas in channels with various geometries, the water forms microscopic droplets. The hydrophobic and hydrophilic properties of the porous media and channel walls control the size and shape of the water droplets.

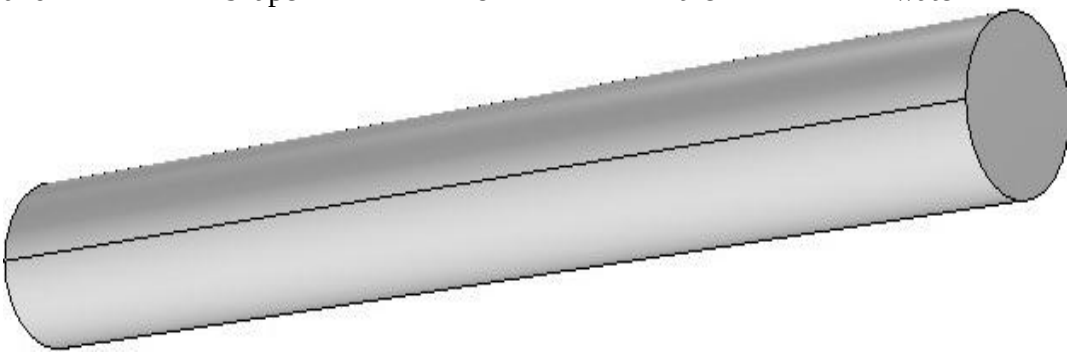

**Fig 1 (a) Cylindrical channel**

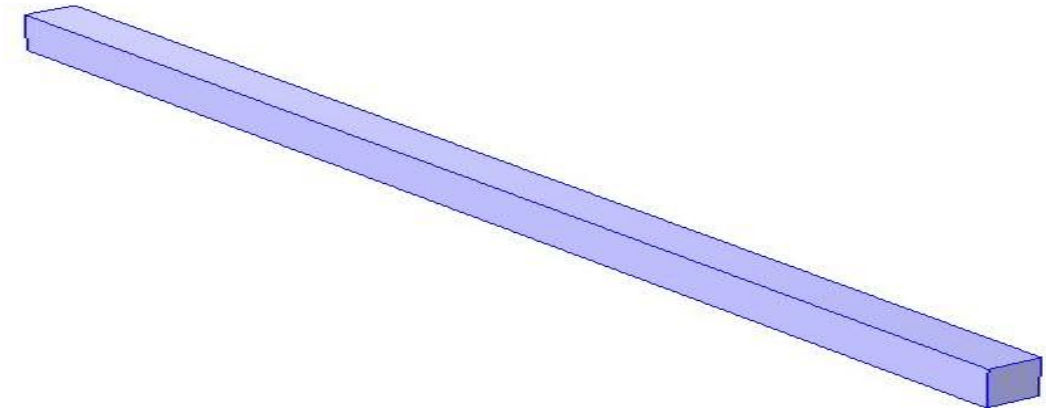

**Fig 1(b) Rectangular channel**

Simulations and Modeling are widely utilized in research institutes to acquire a better knowledge of the underlying mechanisms in these fuel cells, which helps to lower research expenses and improves the design. Numerous studies, models, and computational simulations have been created recently [15–18] to examine a variety of transport processes. The primary goal of this research is to use a 3D model created with COMSOL Multiphysics software to explore the impact of the contact area of the gas flow channel with the GDLs on the performance of the cell.

**Modelling:**

To determine the performance of the PEMFC with membrane, a 3-dimensional single-stage isothermal model is created. In this modeling we have applied electrochemistry module < Hydrogen fuel cell < Proton exchange membrane and two times fluid flow module < Porous media & Subsurface flowfor anode< Free & Porous media flow for cathode.

**Model suppositions:**

Water only occurs in vapor form in the PEMFC when it is operating above 150°C at a pressure of about 1 atm [19]. In contrast to the normal the water drag coefficient from the anode to the cathode is considered to be zero in low temperature PEMFCs using Nafion membranes. due to the nature of PBI membranes [20-22]. Furthermore, the proton transfer mechanism uses the acid in the membrane because it is doped with phosphoric acid [23]. An ideal gas is used to describe a gas mixture. The flow is laminarbecause the Reynolds number is low. Polymers that are homogenous and isotropic are used to create the gas diffusion layer (GDL).

**Modeling domain** —

A portion of the membrane, both cathode and anode GFCs, two catalyst layers, and two GDLs are all included in the 3D computational geometry. Figure 2(a) &2(b) shows seven computational domains of this model.

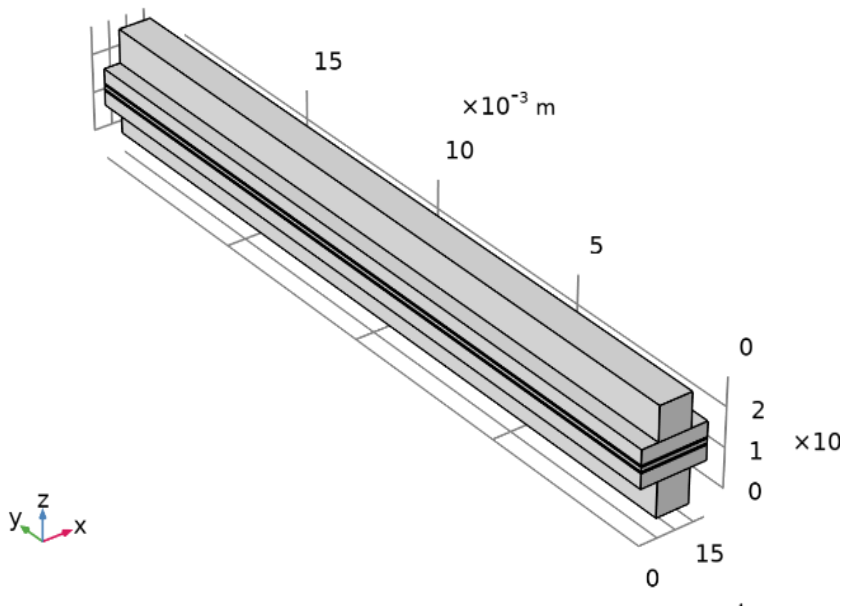


**Fig 2(a) Rectangular channel Geometry of PEMFC**

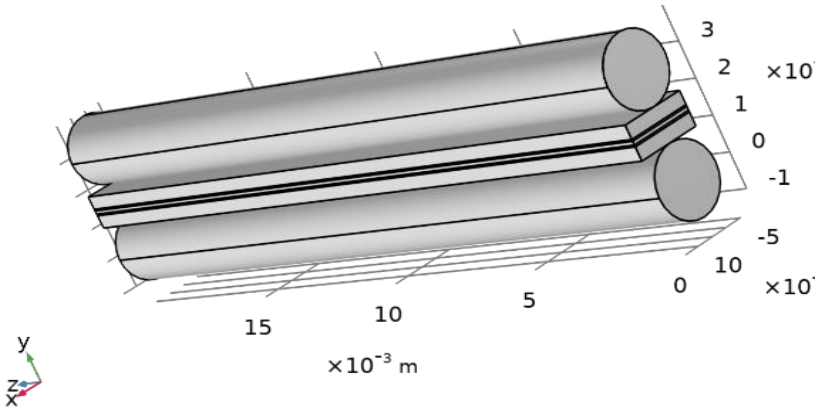


**Fig. 2(b)Cylindrical channel Geometry of PEMFC**

**Governing equations:**

The following conservation equations control the operation of the HT-PEMFC under the assumptions made above.

**Mass Conservation -**

$$\nabla u = \frac{Q}{\rho} \quad (4)$$

Mass transfer to other phases: $Q_m = \sum_i R_i$ (4a)

**Momentum Conservation -**

$$\rho u \cdot \nabla \mathrm{u} = \nabla\{-pI + \mu[\nabla u + (\nabla u)^T]\} \quad (5)$$

$$\mu = \Sigma x_i \cdot \mu_i \quad (5a)$$

The impact of the porous GDL's porosity is taken into consideration by modifying the effective binary diffusivity.

$$\omega_{oj} = \frac{x_{oj} M_i}{M_{n,o}}, \; M_{n,o} = \sum_i x_{oj} M_i \quad (6)$$

$$x_{o,H_2O} = \frac{p_{vap}(T_{hum})}{p_{A,hum}} RH_{hum} \quad (7)$$

$$x_{oj} = x_{oj}\left(1 - x_{O,H_2O}\right) \quad (8)$$

$$D_{ik,eff} = \epsilon_g \; 1.5 D_{ik} \quad (9)$$

**Stefan velocity:**

$$\rho u_s = n \cdot \sum_i (j_i + \rho u_s \omega_i n) \quad (10)$$

In a PEMFC, the current can be divided into two components: ionic current and electronic current [24]. An ionic current is created by the movement of protons viamembrane, as opposed to an electronic current, which exclusively involves the movement of electrons through a solid

electrode matrix. Using Ohm's law, the current continuity equations are generated.

$$\nabla \cdot (-\sigma_s \nabla \cdot \phi_s) = S_s \quad (11a)$$

$$\nabla \cdot (-\sigma_m \nabla \cdot \phi_m) = S_m \quad (11b)$$

Where the phase potential is$\phi$, the effective electric conductivity is $\sigma$ ($S.m^{-1}$), the current source term is S ($A.m^{-3}$), the subscript s stands for the property of the solid phase, and the subscript m stands for the property of the membrane.The source terms for the electron and proton transport equations are produced via the electrochemical reaction, which only occurs in the CLs of the anode and cathode sides [24].$S_m = J_a$ and $S_s = J_a$, and cathode CL, $S_m = J_c$ and $S_s = J_c$. The electrochemical process's transfer current densities at the catalyst layers on the anode and cathode, respectively, are shown here as $J_a$ and $J_c$ [25].

**Constitutive relations**—

The transfer current densities $J_a$ and $J_c$ were estimated using a streamlined Butler-Volmer equation, which is supplied as the source terms in both species and charge equations.

$$J_a = ai_{0,a}^{ref} \left(\frac{C_{H_2}}{C_{H_{2,ref}}}\right)^{0.5} \left(\frac{\alpha_a + \alpha_c}{R_T} F\eta_a\right) \quad (12a)$$

$$J_c = ai_{0,c}^{ref} \left(\frac{C_{O_2}}{C_{O_{2,ref}}}\right)^{0.5} exp\left(-\frac{\alpha_c}{R_T} F\eta_c\right) \quad (12b)$$

Where the potential difference between the electrolyte and the solid matrix is represented by the symbol η and is defined as

Anode side: $\eta_a = \phi_s - \phi_e$ (13a)

Cathode side: $\eta_c = \phi_s - \phi_e - U_{oc}$ (13b)

**Boundary conditions** —

According to the stoichiometric ratio, the active area of FCs, and the GFCs dimensions, the inlet gas velocity is computed and provided as

$$U_{in\_c} = \lambda_c \frac{1}{4F} x_{O_2} \frac{RT}{(P \cdot A_{Channel} \cdot n_{Channel})} \quad (14a)$$

$$U_{in\_a} = \lambda_a \frac{1}{4F} x_{H_2} \frac{RT}{(P \cdot A_{Channel} \cdot n_{Channel})} \quad (14b)$$

$n_{channel}$is the number of the channel, $A_{channel}$ is the channel's cross-sectional area, and $U_{in_c}$and $U_{in_a}$are the average inlet velocities on the cathode and anode sides.

Based on the temperature and humidified air at the entrance, the species fraction is computed. At the flow channel's output, it is set at atmospheric pressure for the back-pressure. The flow is thought to be completely developed. The main plane of the land area's boundary is specified to be symmetrical, and other impermeable walls and surfaces are subject to the no-slip boundary criterion. The fuel cell operating voltage is designed to be the same as the cathode current collector, while changing the anode current collector to zero V. The remaining borders are designed to be insulated or symmetrical.

**Results and discussions**

A complete mess of 13760 domain elements, 5976 boundary elements, and 860 edge elements is used to solve the FC model utilizing the commercial COMSOL Multiphysicssoftware. The solution time is 2187 seconds (36 minute 27 seconds). Numbers of degree of freedoms solved for 105233 plus 9450 internal degrees of freedoms.Geometrical parameters for cylindrical and rectangular (cuboid) shape in table 1.

**Table 1: Modeling parameters**

| S.No. | Parameters Description for cylindrical channel shape | Parameters Description for rectangular channel shape | Value | Parameters Name |
|---|---|---|---|---|
| 1 | L | L | 0.02 m | Cell length |
| 2 | r_ch | - | 0.001 m | Channel radius |
| 3 | Pai_const | - | 22/7 | Pai constant |
| 4 | W_rib | W_rib | 9.0932E-4 m | Rib width |
| 5 | H_gdl | H_gdl | 3.8E-4 m | GDL width |
| 6 | H_electrode | H_electrode | 5E-5 m | Porous electrode thickness |
| 7 | H_membrane | H_membrane | 1E-4 m | Membrane thickness |
| 8 | - | H_ch | 1mm | Channel height |
| 9 | - | W_ch | 0.8mm | Channel width |

**Table 2- Domain probe table for anode gas diffusion electrode for different channel geometry**

| V_cell (V) | Rectangular (Cuboidal)channel current density (mA/cm^2) | Cylindrical channelcurrent density (mA/cm^2) |
|---|---|---|
| 0.95 | 2.78E-04 | 0.00027794 |
| 0.9 | 0.0010248 | 0.0010249 |
| 0.85 | 0.0033023 | 0.0033022 |
| 0.8 | 0.00837 | 0.0083572 |
| 0.7 | 0.027023 | 0.026633 |
| 0.6 | 0.052377 | 0.049741 |
| 0.5 | 0.079568 | 0.068859 |
| 0.4 | 0.10282 | 0.076481 |

The current density expected by the cylindrical channel numerical model was significantly reduced than the actual current density ofrectangular flow channel design.Fig 3 shows the relationship between voltage and current density. This relationship known as polarization curve.

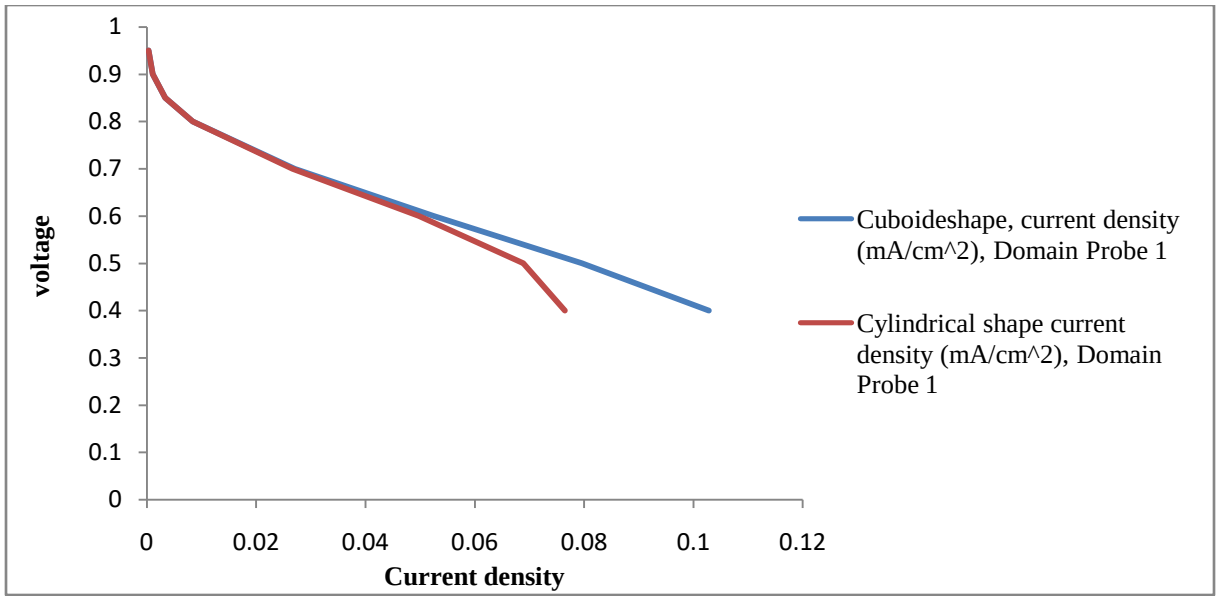


**Fig. 3 Polarization curve between current density and cell voltage**

**Table 3:Comparative results between rectangular and cylindrical channelgeometry**

| Results | Rectangular Channel | Cylindrical Channel |
|---|---|---|
| **Anode compartment Velocity m/s** | 0·2 | $14\times10^{-3}$ |
| **Anode compartment Pressure atm** | -0· 03 | $475{\cdot}29\times10^{-3}$ |
| **Cathode compartment Velocity m/s** | 1 | $8\times10^{-3}$ |
| **Cathode compartment Pressure atm** | 7·29 | $595{\cdot}75\times10^{-3}$ |
| **Membrane Current Density A/cm$^2$** | $1{\cdot}\ 17\times10^{4}$ | $305\times10^{-15}$ |
| **Electrode potential with Respect to GroundV** | 0 · 42 | 0 · 40 |
| **Electrolyte Potential V** | 0 · 35 | 0 · 30 |

## CONCLUSIONS:

In this study, we have drawn rectangular and cylindrical-shaped 3D channel geometries and these geometries have the same area of inlet and outlet of the gas channel due to which the inlet velocity of the gas channel will also be the same. In case rectangular channel geometry PEM fuel cell is generated a high current density (0.10282 mA/cm$^2$). Therefore, the following outcomes based on this research is that performance of ionic current density of the HT-PEMFC is higher ($1{\cdot}\ 17\times10^{4}$) in rectangular channel geometry in the z compartment.Thevelocity magnitude at the cathode compartment is greater in rectangular channel geometry ($1>8\times10^{-3}$). Electrode potential with Respect to Ground in rectangular channel geometry is higher than cylindrical channel geometry (0.42 > 0.40).Electrolyte potential in rectangular channel geometry is higher than cylindrical channel geometry (0.35 > 0.30).

## REFERENCES

**1.** Liu Z. Fuel cell performance. New York: Nova Science Publishers, p.284 (2012).

**2.** A. J. Appleby. From Sir William Grove to today: Fuel cells and the future. Journal of Power Sources, **29**, 3 (1990).

**3.** Hoogers G.; Fuel Cell Technology Handbook, CRC Press. 332 (2002).

**4.** R. Mark Ormerod. Solid oxide fuel cells: Chem. Soc. Rev., **32**, 17 (2003).

**5.** Grime P.; IEEE Aerospace and Electronic Systems Magazine **15** (2) 41 (2000).

**6.** Mond L., Langer C.; A new form of gas battery, Proceeding Royal Society London **46**, 296 (1889).

**7.** Hoogers G. Fuel cell technology handbook. Boca Raton, FL; London: CRC Press. 1 v. (various pagings) [16] p. of plates, (2003).

**8.** Wang Y, Chen KS and Cho SC. PEM fuel cells: thermal and water management fundamentals. New York: Momentum Press, (2013).

**9.** Segura F, Andujar JM, Duran E, Analog Current Control Techniques for Power Control in PEM Fuel-Cell Hybrid Systems: A Critical Review and a Practical Application, IEEE Trans. Ind. Electron. **58**, 1171 (2011).

**10.** Jia J, Wang G, Cham YT, Wang Y, Han M, Electrical Characteristic Study of a Hybrid PEMFC and Ultracapacitor System, IEEE Trans. Ind. Electron. **57**: 1945 (2010).

**11.** Nguyen T V, Water management by material design and engineering for PEM fuel cells, ECS Trans. **3**, 1171 (2006).

**12.** Abtahi H, Zilouchian A, Saengrung A, Water Management of PEM fuel cells using fuzzy logic controller system, 2005 IEEE International Conference on Systems, Man and Cybernetics-SMC, Waikoloa, USA, 3486, (2005).

**13.** Petrone G, Cammarata G, Modelling and Simulation, Croatia: InTeach Education and Publishing; p. 677 (2008).

**14.** Liu Z. Fuel cell performance. New York: Nova Science Publishers, 2012, p.284.

**15.** Viorel Ionescu, Simulating the Effect of Gas Channel Geometry on PEM Fuel Cell Performance by Finite Element Method, Procedia Technology **22**, 713 (2016).

**16.** Zhang J, Xie X, Tang Y, Song C, Navessin T, Shi Z, Song D, Wang H, Wilkinson DP, Liu Z. S, Holdcroft S, High temperature PEM fuel cells, J. Power Sources **160**: 872 (2006).

**17.** Ionescu V, Simulating the effect of gas channel geometry on PEM fuel cell performance by finite element method, Procedia Technology; **22** (2016).

**18.** Kone J P, Zhang X, Yan Y, Hu G and Ahmadi G, Three-dimensional multiphase flow computational fluid dynamics models for proton exchange membrane fuel cell: A theoretical development, The Journal of Computational Multiphase Flows **9** (1) 3 (2017).

**19.** Schmidt T. J. and Baurmeister J., Properties of high-temperature PEFC Celtec®-1000 MEAs in start/stop operation mode, J. Power Sources, **176**, 428 (2008).

**20.** Zhang J., Tang Y., Song C., and Zhang J., Polybenzimidazole-membrane-based PEM fuel cell in the temperature range of 120–200 °C, J. Power Sources, **172**, 163 (2007).

**21.** Weng D., Wainright J. S., Landau U., and Savinell R. F.; Electro-osmotic Drag Coefficient of Water and Methanol inPolymer Electrolytes at Elevated TemperaturesJ. Electrochem. Soc., **143**, 1260 (1996).

**22.** Ren X., Henderson W. and Gottesfeld S., Electro-osmotic Drag of Water in Ionomeric Membranes: New Measurements Employing a Direct Methanol Fuel Cell, J. Electrochem. Soc., **144**, L267 (1997).

**23.** Incropera F. P., DeWitt D. P., Fundamentals of Heat and Mass Transfer, John Wiley & Sons, New York 1996.

**24.** IonescuV. High temperature PEM fuel cell steady-state transport modeling. Ovidius University Annals of Chemistry **24** (1), 55 (2013).

**25.** T. Zhang et al. Combination effects of flow field structure and assembly force on performance of high temperature proton exchange membrane fuel cells. Int J Energy Res. **45**, 7903 (2021).